

HMXB and LMXB evolution and their links with gravitational wave sources

Dynamical versus isolated formation channels of gravitational wave sources

Michela Mapelli^{1,2,3,4}

¹Dipartimento di Fisica e Astronomia G. Galilei, Università degli Studi di Padova, Vicolo dell'Osservatorio 3, I-35122, Padova, Italy
email: michela.mapelli@unipd.it

²Institut für Astro- und Teilchenphysik, Universität Innsbruck, Technikerstrasse 25/8, A-6020 Innsbruck, Austria

³INAF – Osservatorio Astronomico di Padova, Vicolo dell'Osservatorio 5, I-35142 Padova, Italy

⁴INFN – Sezione di Padova, Via F. Marzolo 8, I-35131 Padova, Italy

Abstract. What are the formation channels of merging black holes and neutron stars? The first two observing runs of Advanced LIGO and Virgo give us invaluable insights to address this question, but a new approach to theoretical models is required, in order to match the challenges posed by the new data. In this review, I discuss the impact of stellar winds, core-collapse and pair instability supernovae on the formation of compact remnants in both isolated and dynamically formed binaries. Finally, I show that dynamical processes, such as the runaway collision scenario and the Kozai-Lidov mechanism, leave a clear imprint on the demography of merging systems.

Keywords. black hole physics – gravitational waves – (stars:) binaries: general – stellar dynamics – stars: winds – galaxies: star clusters

1. Lesson learned from the first direct gravitational wave detections

On September 14 2015, the LIGO interferometers captured a gravitational wave (GW) signal from two merging black holes (BHs, [Abbott *et al.* 2016a](#)). This event, named GW150914, is the first direct detection of GWs, about hundred years after Einstein's prediction. To date, nine more BH mergers have been reported (GW151012, GW151226, GW170104, GW170608, GW170729, GW170809, GW170814, GW170818 and GW17082 [Abbott *et al.* 2016b,c, 2017a,c,b, 2018a,b](#)). In particular, GW170814 was the first BH merger detected jointly by three interferometers: the two LIGO detectors in the United States ([Aasi *et al.* 2015](#)) and Virgo in Italy ([Acernese *et al.* 2015](#)).

Astrophysicists have learned several revolutionary concepts about BHs from GW detections ([Abbott *et al.* 2016d](#)). First, GW150914 has confirmed the existence of double BH binaries (BHBs), i.e. binaries composed of two BHs. BHBs have been predicted a long time ago (e.g. [Tutukov & Yungelson 1973](#); [Thorne 1987](#); [Schutz 1989](#); [Kulkarni *et al.* 1993](#); [Sigurdsson *et al.* 1993](#); [Bethe & Brown 1998](#); [Portegies Zwart & McMillan 2000](#); [Colpi *et al.* 2003](#); [Belczynski *et al.* 2004](#)), but their observational confirmation was still missing. Second, GW detections show that some BHBs are able to merge within a Hubble time.

Finally, seven out of ten merging BHBs detected so far host BHs with mass in excess of $30 M_{\odot}$. This result was a genuine surprise for the astrophysicists, because the only stellar BHs for which we have a dynamical mass measurement, i.e. about a dozen of BHs in X-ray binaries, have mass $< 20 M_{\odot}$ (see [Figure 1](#) for a compilation of measured BH

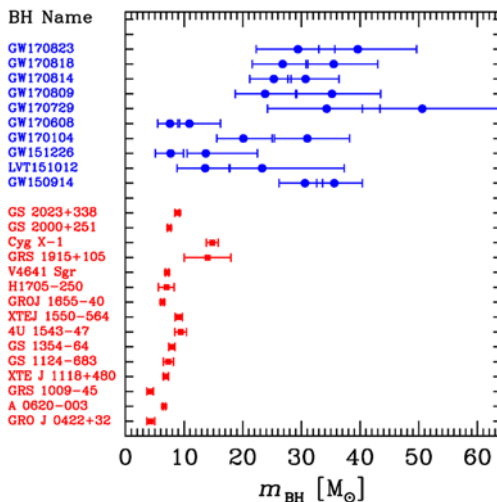


Figure 1. A compilation of BH masses m_{BH} from observations. Red squares: BHs with dynamical mass measurement in X-ray binaries (Orosz *et al.* 2003; Özel *et al.* 2010). This selected sample is quite conservative, because uncertain and debated results are not being shown (e.g. IC10 X-1 Laycock *et al.* 2015). Blue circles: BHs in the first published GW events (Abbott *et al.* 2016c, 2017a,b, 2018a,b).

masses). Moreover, most theoretical models did not predict the existence of BHs with mass $m_{\text{BH}} > 30 M_{\odot}$ (but see Mapelli *et al.* 2009, 2010, 2013; Belczynski *et al.* 2010; Fryer *et al.* 2012; Ziosi *et al.* 2014; Spera *et al.* 2015 for several exceptions). Thus, the first GW detections have urged the astrophysical community to deeply revise the models of BH formation and evolution.

2. The formation of compact remnants from stellar evolution and supernova explosions

BHs and neutron stars (NSs) are expected to form as compact relics of massive ($\gtrsim 8 M_{\odot}$) stars. An alternative theory predicts that BHs can form also from gravitational collapse in the early Universe (the so called primordial BHs, e.g. Bird *et al.* 2016; Carr *et al.* 2016; Inomata *et al.* 2016). In this review, we will focus on BHs of stellar origin.

The mass function of BHs is highly uncertain, because it may be affected by a number of barely understood processes. In particular, stellar winds and supernova (SN) explosions both play a major role on the formation of compact remnants. Processes occurring in close binary systems (e.g. mass transfer and common envelope) are a further complication and will be discussed in the next section.

2.1. Stellar winds and stellar evolution

Stellar winds are outflows of gas from the atmosphere of a star. In cold stars (e.g. red giants and asymptotic giant branch stars) they are mainly induced by radiation pressure on dust, which forms in the cold outer layers (e.g. van Loon *et al.* 2005). In massive hot stars (O and B main sequence stars, luminous blue variables and Wolf-Rayet stars), stellar winds are powered by the coupling between the momentum of photons and that of metal ions present in the stellar photosphere. A large number of strong and weak resonant metal lines are responsible for this coupling.

Understanding stellar winds is tremendously important for the study of compact objects, because mass loss determines the pre-SN mass of a star (both its total mass and its core mass), which in turn affects the outcome of an SN explosion (Fryer *et al.* 1999; Fryer & Kalogera 2001; Mapelli *et al.* 2009, 2010; Belczynski *et al.* 2010).

Early work on stellar winds (e.g. Abbott 1982; Kudritzki *et al.* 1987; Leitherer *et al.* 1992) highlighted that the mass loss of O and B stars depends on metallicity as $\dot{m} \propto Z^\alpha$ (with $\alpha \sim 0.5 - 1.0$, depending on the model). However, such early work did not account for multiple scattering, i.e. for the possibility that a photon interacts several times before being absorbed or leaving the photosphere. Vink *et al.* (2001) accounted for multiple scatterings and found a universal metallicity dependence $\dot{m} \propto Z^{0.85} v_\infty^p$, where v_∞ is the terminal velocity[†] and $p = -1.23$ ($p = -1.60$) for stars with effective temperature $T_{\text{eff}} \gtrsim 25000$ K (12000 K $\lesssim T_{\text{eff}} \lesssim 25000$ K).

The situation is more uncertain for post-main sequence stars. For Wolf-Rayet (WR) stars, i.e. naked Helium cores, Vink & de Koter (2005) predict a similar trend with metallicity $\dot{m} \propto Z^{0.86}$. Hainich *et al.* (2015) find an even stronger dependence on metallicity (see their Figures 10 and 11), based on a quantitative analysis of several Wolf-Rayet N stars in the Local Group performed with the Potsdam Wolf-Rayet model atmosphere code.

With a different approach (which accounts also for wind clumping), Gräfener & Hamann (2008) find a strong dependence of WR mass loss on metallicity but also on the electron-scattering Eddington factor $\Gamma_e = \kappa_e L / (4 \pi c G m)$, where κ_e is the cross section for electron scattering, L is the stellar luminosity, c is the speed of light, G is the gravity constant, and m is the stellar mass. The importance of Γ_e has become increasingly clear in the last few years (Gräfener *et al.* 2011; Vink *et al.* 2011), but, unfortunately, only few stellar evolution models include this effect. For example, Chen *et al.* (2015) adopt a mass loss prescriptions $\dot{m} \propto Z^\alpha$, where $\alpha = 0.85$ if $\Gamma_e < 2/3$ and $\alpha = 2.45 - 2.4 \Gamma_e$ if $2/3 \leq \Gamma_e \leq 1$. This simple formula accounts for the fact that metallicity dependence tends to vanish when the star is close to be radiation pressure dominated.

2.2. Supernovae (SNe)

The mechanisms triggering iron core-collapse SNe are still highly uncertain. Several mechanisms have been proposed, including rotationally-driven SNe and/or magnetically-driven SNe (see e.g. Janka 2012; Foglizzo *et al.* 2015 and references therein). The most commonly investigated mechanism is the convective SN engine (see e.g. Fryer *et al.* 2012).

Fully self-consistent simulations of core collapse with a state-of-the-art treatment of neutrino transport do not lead to explosions in spherical symmetry except for the lighter SN progenitors ($\lesssim 10 M_\odot$, Foglizzo *et al.* 2015; Ertl *et al.* 2016). Simulations which do not require the assumption of spherical symmetry (i.e. run at least in 2D) appear to produce successful explosions from first principles for a larger range of progenitor masses (see e.g. Müller & Janka *et al.* 2012a,b). However, 2D and 3D simulations are still computationally challenging and cannot be used to make a study of the mass distribution of compact remnants.

Thus, in order to study compact-object masses, SN explosions are artificially induced by injecting in the pre-SN model some amount of kinetic energy (kinetic bomb) or thermal

[†] The terminal velocity v_∞ is the the velocity reached by the wind at large distance from the star, where the radiative acceleration approaches zero because of the geometrical dilution of the photospheric radiation field. Since line-driven winds are continuously accelerated by the absorption of photospheric photons in spectral lines, v_∞ corresponds to the maximum velocity of the stellar wind. See the review by Kudritzki (2000) for more details.

energy (thermal bomb) at an arbitrary mass location. The evolution of the shock is then followed by means of 1D hydrodynamical simulations with some relatively simplified treatment for neutrinos. This allows to simulate hundreds of stellar models.

Following this approach, O'Connor & Ott (2011) propose a criterion to decide whether a SN is successful or not, based on the compactness parameter:

$$\xi_m = \frac{m/M_\odot}{R(m)/1000 \text{ km}}, \quad (2.1)$$

where $R(m)$ is the radius which encloses a given mass m . Usually, the compactness is defined for $m = 2.5 M_\odot$ ($\xi_{2.5}$). O'Connor & Ott (2011) measure the compactness at core bounce[†] in their simulations and find that the larger $\xi_{2.5}$ is, the shorter the time to form a BH (as shown in their Figure 6). This means that stars with a larger value of $\xi_{2.5}$ are more likely to collapse to a BH without SN explosion. The work by Ugliano *et al.* (2012) and Horiuchi *et al.* (2014) indicate that the best threshold between exploding and non-exploding models is $\xi_{2.5} \sim 0.2$.

The models proposed by O'Connor & Ott (2011) (see also Ertl *et al.* 2016; Sukhbold *et al.* 2014, 2016) are sometimes referred to as the “islands of explodability” scenario, because they predict a non-monotonic behaviour of SN explosions with the stellar mass. This means, for example, that while a star with a mass $m = 25 M_\odot$ and a star with a mass $m = 29 M_\odot$ might end their life with a powerful SN explosion, another star with intermediate mass between these two (e.g. with a mass $m = 27 M_\odot$) is expected to directly collapse to a BH without SN explosion. Thus, these models predict the existence of “islands of explodability”, i.e. ranges of mass where a star is expected to explode, surrounded by mass intervals in which the star will end its life with a direct collapse.

Finally, it is important to recall pair-instability and pulsational pair-instability SNe (Fowler *et al.* 1964; Barkat *et al.* 1967; Rakavy *et al.* 1967; Woosley 2017). If the Helium core of a star grows above $\sim 30 M_\odot$ and the core temperature is $\gtrsim 7 \times 10^8$ K, the process of electron-positron pair production becomes effective. It removes photon pressure from the core producing a sudden collapse before the iron core is formed. For $m_{\text{He}} > 135 M_\odot$, the collapse cannot be reversed and the star collapses directly in to a BH (Woosley 2017). If $135 \gtrsim m_{\text{He}} \gtrsim 64 M_\odot$, the collapse triggers an explosive burning of heavier elements, which has disruptive effects. This leads to a complete disruption of the star, leaving no remnant (the so-called pair-instability SN, Heger & Woosley 2002).

For $64 \gtrsim m_{\text{He}} \gtrsim 32 M_\odot$, pair production induces a series of pulsations of the core (pulsational pair instability SNe), which trigger an enhanced mass loss (Woosley 2017). At the end of this instability phase a remnant with non-zero mass is produced, significantly lighter than in case of a direct collapse.

2.3. The mass of compact remnants

The previous sections suggest that our knowledge of compact object mass is hampered by severe uncertainties, connected with both stellar winds and core-collapse SNe. Thus, models of the mass spectrum of compact remnants must be taken with a grain of salt. However, few robust features can be drawn.

Figure 2 is a simplified version of Figures 2 and 3 of (Heger *et al.* 2003). The final mass of a star and the mass of the compact remnant are shown as a function of the ZAMS mass. The left and the right-hand panels show the case of a solar metallicity star and of a metal-free star, respectively. In the case of the solar metallicity star, the final mass of the

[†] Ugliano *et al.* (2012) show that $\xi_{2.5}$ is not significantly different at core bounce or at the onset of collapse.

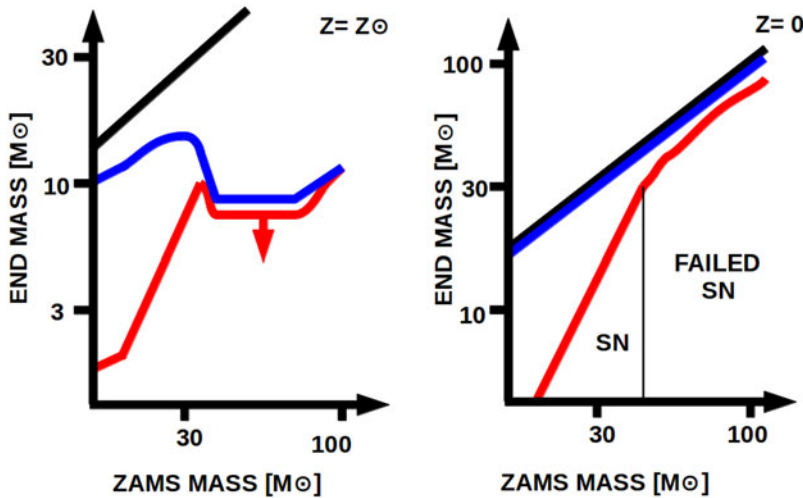


Figure 2. Final mass of a star (m_{fin} , blue lines) and mass of the compact remnant (m_{rem} , red lines) as a function of the ZAMS mass of the star. The thick black line marks the region where $m_{\text{fin}} = m_{\text{ZAMS}}$. Left-hand panel: solar metallicity star. Right-hand panel: metal-free star. The red arrow on the left-hand panel is an upper limit for the remnant mass. Vertical thin black line in the right-hand panel: approximate separation between successful and failed SNe at $Z = 0$. This cartoon was inspired by Figures 2 and 3 of Heger *et al.* (2003).

star is much lower than the initial one, because stellar winds are extremely efficient. The mass of the compact object is also much lower than the final mass of the star because a core-collapse SN always takes place.

In contrast, a metal-free star (i.e. a population III star) loses a negligible fraction of its mass by stellar winds (the blue and the black line in Figure 2 are superimposed). As for the mass of the compact remnant, Figure 2 shows that there are two regimes: below a given threshold ($\approx 30 - 40 M_{\odot}$) the SN explosion succeeds even at zero metallicity and the mass of the compact remnant is relatively small. Above this threshold, the mass of the star (in terms of both core mass and envelope mass) is sufficiently large that the SN fails. Most of the final stellar mass collapses to a BH, whose mass is significantly larger than in the case of a SN explosion.

What happens at intermediate metallicity between solar and zero, i.e. in the vast majority of the Universe we know?

As a rule of thumb (see e.g. Fryer *et al.* 2012; Spera *et al.* 2015), we can draw the following considerations. If the zero-age main sequence (ZAMS) mass of a star is large ($m_{\text{ZAMS}} \gtrsim 30 M_{\odot}$), then the amount of mass lost by stellar winds is the main effect which determines the mass of the compact object. At low metallicity ($\lesssim 0.1 Z_{\odot}$) and for a low Eddington factor ($\Gamma_e < 0.6$), mass loss by stellar winds is not particularly large. Thus, the final mass m_{fin} and the compactness $\xi_{2.5}$ of the star may be sufficiently large to avoid a core-collapse SN explosion: the star may form a massive BH ($\gtrsim 20 M_{\odot}$) by direct collapse, unless a pair-instability or a pulsational-pair instability SN occurs. At high metallicity ($\approx Z_{\odot}$) or large Eddington factor ($\Gamma_e > 0.6$), mass loss by stellar winds is particularly efficient and may lead to a small m_{fin} : the star is expected to undergo a core-collapse SN and to leave a relatively small compact object.

If the ZAMS mass of a star is relatively low ($7 < m_{\text{ZAMS}} < 30 M_{\odot}$), then stellar winds are not important (with the exception of super asymptotic giant branch stars), regardless of the metallicity. In this case, the details of the SN explosion (e.g. energy of the explosion and amount of fallback) are crucial to determine the final mass of the compact object.

This general sketch may be affected by several factors, such as pair-instability SNe, pulsational pair-instability SNe (e.g. Woosley 2017) and an *island scenario* for core-collapse SNe (e.g. Ertl *et al.* 2016).

The effect of pair-instability and pulsational pair-instability SNe is clearly shown in Figure 3. The top panel was obtained accounting only for stellar evolution and core-collapse SNe. In contrast, the bottom panel also includes pair-instability and pulsational pair-instability SNe. This figure shows that the mass of the compact remnant strongly depends on the metallicity of the progenitor star if $m_{\text{ZAMS}} \gtrsim 30 M_{\odot}$. In most cases, the lower the metallicity of the progenitor is, the larger the maximum mass of the compact remnant (Heger *et al.* 2003; Mapelli *et al.* 2009; Belczynski *et al.* 2010; Mapelli *et al.* 2010, 2013; Spera *et al.* 2015; Spera & Mapelli 2017). However, for metal-poor stars ($Z < 10^{-3}$) with ZAMS mass $230 > m_{\text{ZAMS}} > 110 M_{\odot}$ pair instability SNe lead to the complete disruption of the star and no compact object is left. Only very massive ($m_{\text{ZAMS}} > 230 M_{\odot}$) metal-poor ($Z < 10^{-3}$) stars can collapse to a BH directly, producing intermediate-mass BHs (i.e. BHs with mass $\gtrsim 100 M_{\odot}$).

If $Z < 10^{-3}$ and $110 > m_{\text{ZAMS}} \gtrsim 60 M_{\odot}$, the star enters the pulsational pair-instability SN regime: mass loss is enhanced and the final BH mass is smaller ($m_{\text{BH}} \sim 30 - 55 M_{\odot}$, bottom panel of Fig. 3) than we would have expected from direct collapse ($m_{\text{BH}} \sim 50 - 100 M_{\odot}$, top panel of Fig. 3). Thus, accounting for both pair instability and pulsational pair-instability SNe leads to a *BH mass gap*† between $m_{\text{BH}} \sim 60 M_{\odot}$ and $m_{\text{BH}} \sim 120 M_{\odot}$.

3. Binaries of stellar black holes

Naively, one could think that if two massive stars are members of a binary system, they will eventually become a double BH binary and the mass of each BH will be the same as if its progenitor star was a single star. This is true only if the binary system is sufficiently wide (detached binary) for its entire evolution. If the binary is close enough, it will evolve through several processes which might significantly change its final fate.

The so-called binary population-synthesis codes have been used to investigate the effect of binary evolution processes on the formation of BHBs in isolated binaries (e.g. (Portegies Zwart *et al.* 1996; Hurley *et al.* 2002; Podsiadlowski *et al.* 2003; Belczynski *et al.* 2008; Mapelli *et al.* 2013; Mennekens *et al.* 2014; Eldridge *et al.* 2016; Mapelli *et al.* 2017; Stevenson *et al.* 2017; Giacobbo *et al.* 2018; Barrett *et al.* 2018; Giacobbo *et al.* 2018b; Kruckow *et al.* 2018; Eldridge *et al.* 2018; Mapelli & Giacobbo 2018; Spera *et al.* 2018; Giacobbo *et al.* 2019)). These are Monte-Carlo based codes which combine a description of stellar evolution with prescriptions for supernova explosions and with a formalism for binary evolution processes.

In the following, we mention some of the most important binary-evolution processes and we briefly discuss their treatment in the most used population-synthesis codes.

3.1. Mass transfer

If two stars exchange matter to each other, it means they undergo a mass transfer episode.

The Roche lobe of a star in a binary system is the maximum equipotential surface around the star within which matter is bound to the star. While the exact shape of

† The existence of a BH mass gap between ~ 50 and $\sim 100 M_{\odot}$ is currently consistent with GW detections (see e.g. Fishbach *et al.* (2017); Talbot *et al.* (2018); Wysocki *et al.* (2018); Abbott *et al.* (2018b)).

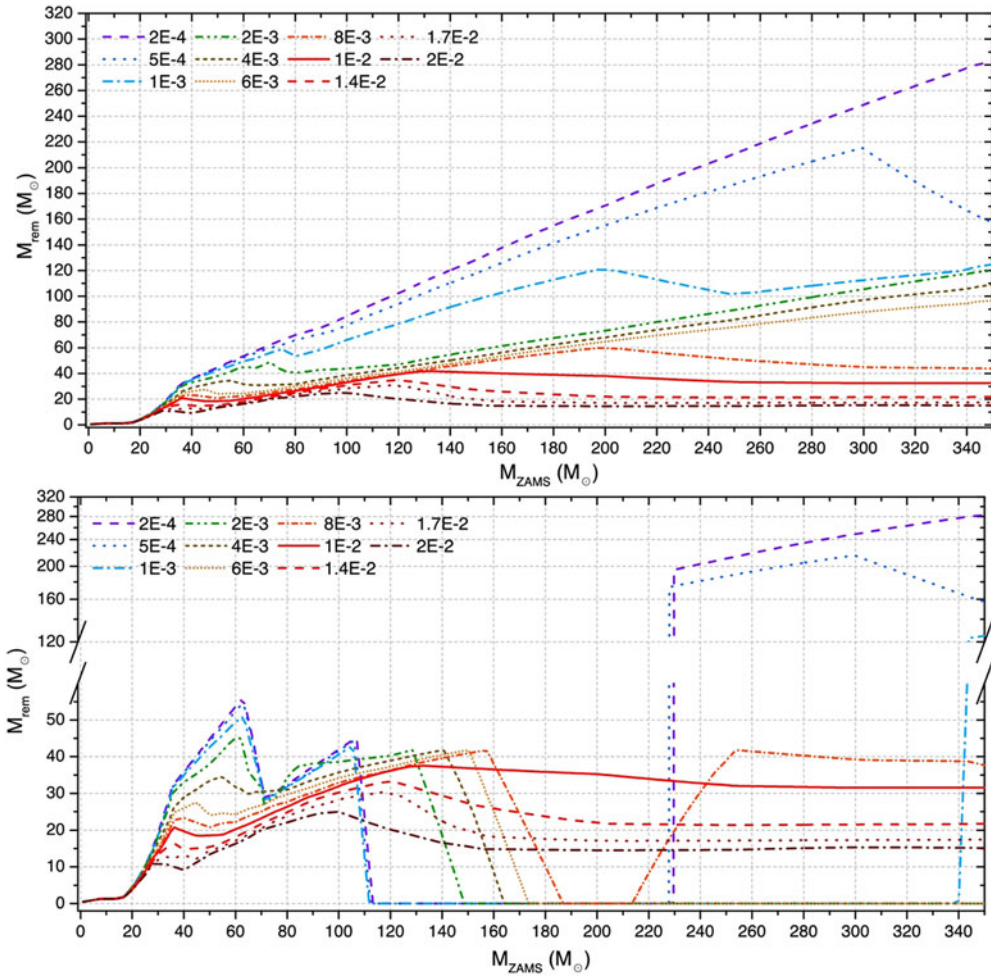


Figure 3. Mass of the compact remnant (m_{rem}) as a function of the ZAMS mass of the star (m_{ZAMS}). Lower (upper) panel: pulsational pair-instability and pair-instability SNe are (are not) included. In both panels: dash-dotted brown line: $Z = 2.0 \times 10^{-2}$; dotted dark orange line: $Z = 1.7 \times 10^{-2}$; dashed red line: $Z = 1.4 \times 10^{-2}$; solid red line: $Z = 1.0 \times 10^{-2}$; short dash-dotted orange line: $Z = 8.0 \times 10^{-3}$; short dotted light orange line: $Z = 6.0 \times 10^{-3}$; short dashed green line: $Z = 4.0 \times 10^{-3}$; dash-double dotted green line: $Z = 2.0 \times 10^{-3}$; dash-dotted light blue line: $Z = 1.0 \times 10^{-3}$; dotted blue line: $Z = 5.0 \times 10^{-4}$; dashed violet line: $Z = 2.0 \times 10^{-4}$. A delayed core-collapse SN mechanism has been assumed, following the prescriptions of (Fryer *et al.* 2012). This Figure was adapted from Figures 1 and 2 of Spera & Mapelli (2017).

the Roche lobe should be calculated numerically, a widely used approximate formula Eggleton (1993) is

$$r_{\text{L},1} = a \frac{0.49 q^{2/3}}{0.6 q^{2/3} + \ln(1 + q^{1/3})}, \quad (3.1)$$

where a is the semi-major axis of the binary and $q = m_1/m_2$ (m_1 and m_2 are the masses of the two stars in the binary). This formula describes the Roche lobe of star with mass m_1 , while the corresponding Roche lobe of star with mass m_2 ($r_{\text{L},2}$) is obtained by swapping the indexes.

The Roche lobes of the two stars in a binary are thus connected by the L1 Lagrangian point. Since the Roche lobes are equipotential surfaces, matter orbiting at or beyond the Roche lobe can flow freely from one star to the other. We say that a star overfills (under-fills) its Roche lobe when its radius is larger (smaller) than the Roche lobe. If a star overfills its Roche lobe, a part of its mass flows toward the companion star which can accrete (a part of) it. The former and the latter are thus called donor and accretor star, respectively.

Mass transfer obviously changes the mass of the two stars in a binary, and thus the final mass of the compact objects, but also the orbital properties of the binary. If mass transfer is non conservative (which is the most realistic case in both mass transfer by stellar winds and Roche lobe overflow), it leads to an angular momentum loss, which in turn affects the semi-major axis.

If mass transfer is dynamically unstable or both stars overfill their Roche lobe, then the binary is expected to merge – if the donor lacks a steep density gradient between the core and the envelope –, or to enter common envelope (CE) – if the donor has a clear distinction between core and envelope.

3.2. Common envelope (CE)

If two stars enter in CE, their envelope(s) stop co-rotating with their cores. The two stellar cores (or the compact remnant and the core of the star, if the binary is already single degenerate) are embedded in the same non-corotating envelope and start spiralling in as an effect of gas drag exerted by the envelope. Part of the orbital energy lost by the cores as an effect of this drag is likely converted into heating of the envelope, making it more loosely bound. If this process leads to the ejection of the envelope, then the binary survives, but the post-CE binary is composed of two naked stellar cores (or a compact object and a naked stellar core). Moreover, the orbital separation of the two cores (or the orbital separation of the compact object and the core) is considerably smaller than the initial orbital separation of the binary, as an effect of the spiral in[†]. This circumstance is crucial for the fate of a BH binary. In fact, if the binary which survives a CE phase evolves into a double BH binary, this double BH binary will have a very short semi-major axis, much shorter than the sum of the maximum radii of the progenitor stars, and may be able to merge by GW emission within a Hubble time.

In contrast, if the envelope is not ejected, the two cores (or the compact object and the core) spiral in till they eventually merge. This premature merger of a binary during a CE phase prevents the binary from evolving into a double BH binary.

The $\alpha\lambda$ formalism (Webbink 1984) is the most common formalism adopted to describe a common envelope. The basic idea of this formalism is that the energy needed to unbind the envelope comes uniquely from the loss of orbital energy of the two cores during the spiral in. This formalism relies on two free parameters, α , which describes the conversion efficiency of orbital energy into thermal energy ($\alpha = E_{\text{th}}/E_{\text{b}} \leq 1$, where E_{b} and E_{th} are the binding energy of the two cores and the thermal energy acquired by the envelope as an effect of the spiral-in, respectively), and λ , describing the concentration of the halo. Actually, we have known for a long time (see Ivanova *et al.* 2013 for a review) that this simple formalism is a poor description of the physics of CE, which is considerably more complicated. For example, there is a number of observed systems for which an $\alpha > 1$ is

[†] Note that a short-period (from few hours to few days) binary system composed of a naked Helium core and BH might be observed as an X-ray binary, typically a Wolf-Rayet X-ray binary. In the local Universe, we know a few (~ 7) Wolf-Rayet X-ray binaries, in which a compact object (BH or NS) accretes mass through the wind of the naked stellar companion (see e.g. Esposito *et al.* 2015 for more details). These rare X-ray binaries are thought to be good progenitors of merging compact-object binaries.

required, which is obviously un-physical. Moreover, λ cannot be the same for all stars. It is expected to vary wildly not only from star to star but also during different evolutionary stages of the same star. Thus, it would be extremely important to model the CE in detail, for example with numerical simulations. A lot of effort has been put on this in the last few years, but there are still many open questions.

3.3. *Alternative evolution to CE*

Massive fast rotating stars can have a chemically homogeneous evolution (CHE): they do not develop a chemical composition gradient because of the mixing induced by rotation. This is particularly true if the star is metal poor, because stellar winds are not efficient in removing angular momentum. If a binary is very close, the spins of its members are even increased during stellar life, because of tidal synchronisation. The radii of stars following CHE are usually much smaller than the radii of stars developing a chemical composition gradient (de Mink & Mandel 2016; Mandel & de Mink 2016). This implies that even very close binaries (few tens of solar radii) can avoid CE.

Marchant *et al.* (2016) simulate very close binaries whose components are fast rotating massive stars. A number of their simulated binaries evolve into contact binaries where both binary components fill and even overflow their Roche volumes. If metallicity is sufficiently low and rotation sufficiently fast, these binaries may evolve as “over-contact” binaries[†]: the over-contact phase differs from a classical CE phase because co-rotation can, in principle, be maintained as long as material does not overflow the L2 point. This means that a spiral-in that is due to viscous drag can be avoided, resulting in a stable system evolving on a nuclear timescale.

Such over-contact binaries maintain relatively small stellar radii during their evolution (few ten solar radii) and may evolve into a double BH binary with a very short orbital period. This scenario predicts the formation of merging BHs with relatively large masses ($> 20 M_{\odot}$), nearly equal mass ($q = 1$), and with large aligned spins.

3.4. *Summary of the isolated binary formation channel*

In this section, we have highlighted the most important aspects and the open issues of the “isolated binary formation scenario”, i.e. the model which predicts the formation of merging BHs through the evolution of isolated binaries. For isolated binaries we mean stellar systems which are not perturbed by other stars or compact objects.

To summarize, let us illustrate schematically the evolution of an isolated stellar binary (see e.g. Belczynski *et al.* 2016; Mapelli *et al.* 2017; Stevenson *et al.* 2017; Giacobbo *et al.* 2018) which can give birth to merging BHs like GW150914 and the other massive BHs observed by the LIGO-Virgo collaboration (Abbott *et al.* 2016a,c, 2017a,b, 2018a). In the following discussion, several details of stellar evolution have been simplified or skipped to facilitate the reading for non specialists.

The left-hand panel of Figure 4 shows the evolution of an isolated binary system composed of two massive stars. These stars are gravitationally bound since their birth. Initially, the two stars are both on the main sequence (MS). When the most massive one leaves the MS (i.e. when Hydrogen burning in the core is over, which happens usually on a time-scale of few Myr for massive stars with ZAMS mass $m_{\text{ZAMS}} \gtrsim 30 M_{\odot}$), its radius starts inflating and can grow by a factor of a hundreds. The most massive star becomes a giant star with a Helium core and a large Hydrogen envelope. If its radius equals the Roche lobe (equation 3.1), the system starts a stable mass-transfer episode. Some mass is lost by the system, some is transferred to the companion. After several additional

[†] It is interesting to note that Hainich *et al.* (2018) actually show that the parameters required for over-compact binaries exist in observed stellar populations.

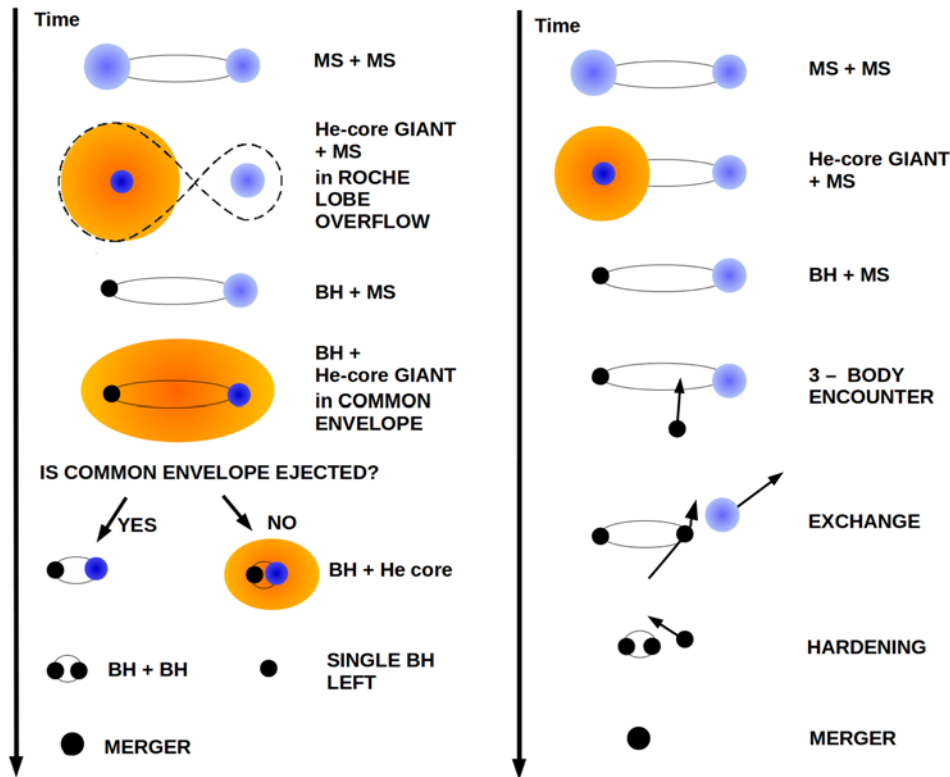


Figure 4. Left: Schematic evolution of an isolated binary which can give birth to a merging BH (see e.g. [Belczynski *et al.* 2016](#); [Mapelli *et al.* 2017](#); [Stevenson *et al.* 2017](#); [Giacobbo *et al.* 2018](#)). Right: Schematic evolution of a merging BHB formed by dynamical exchange (see e.g. [Downing *et al.* 2010](#); [Ziosi *et al.* 2014](#); [Mapelli 2016](#); [Rodríguez *et al.* 2015, 2016](#); [Askar *et al.* 2017](#)).

evolutionary stages, the primary collapses to a BH (a direct collapse is preferred with respect to a SN explosion if we want the BH to be rather massive). At this stage the system is still quite large (hundreds to thousands of solar radii).

When also the secondary leaves the MS, growing in radius, the system enters a CE phase: the BH and the Helium core spiral in. If the orbital energy is not sufficient to unbind the envelope, then the BH merges with the Helium core leaving a single BH. In contrast, if the envelope is ejected, we are left with a new binary, composed of the BH and of a stripped naked Helium star. The new binary has a much smaller orbital separation (tens of solar radii) than the pre-CE binary, because of the spiral-in. If this new binary remains bound after the naked Helium star undergoes a SN explosion or if the naked Helium star is sufficiently massive to directly collapse to a BH, the system evolves into a close BHB, which might merge within a Hubble time.

The most critical quantities in this scenario are the masses of the two stars and also their initial separation (with respect to the stellar radii): a BHB can merge within a Hubble time only if its initial orbital separation is tremendously small (few tens of solar radii, unless the eccentricity is rather extreme); but a massive star ($> 20 M_{\odot}$) can reach a radius of several thousand solar radii during its evolution. Thus, if the initial orbital separation of the stellar binary is tens of solar radii, the binary merges before it can become a BHB. On the other hand, if the initial orbital separation is too large, the two BHs will never merge. In this scenario, the two BHs can merge only if the initial orbital

separation of the progenitor stellar binary is in the range which allows the binary to enter CE and then to leave a short period BHB. This range of initial orbital separations dramatically depends on CE efficiency and on the details of stellar mass and radius evolution.

4. The dynamics of black hole binaries

In the previous sections of this review, we discussed the formation of BH binaries as isolated binaries. There is an alternative channel for BH binary formation: the dynamical evolution scenario.

4.1. Dynamically active environments

Collisional dynamics is important for the evolution of binaries only if they are in a dense environment ($\gtrsim 10^3$ stars pc $^{-3}$), such as a star cluster. On the other hand, astrophysicists believe that the vast majority of massive stars (which are BH progenitors) form in star clusters (Lada & Lada 2003; Weidner *et al.* 2006, 2010; Portegies Zwart *et al.* 2010).

Most studies of dynamical formation of BH binaries focus on globular clusters (e.g. Sigurdsson *et al.* 1993; Portegies Zwart & McMillan 2000; Mapelli *et al.* 2005; Downing *et al.* 2010; Benacquista 2013; Samsing *et al.* 2014; Rodriguez *et al.* 2015, 2016; Askar *et al.* 2017; Samsing *et al.* 2017). *Globular clusters* are old stellar systems (~ 12 Gyr), mostly very massive ($> 10^4 M_{\odot}$) and dense ($> 10^4 M_{\odot}$ pc $^{-3}$). They are sites of intense dynamical processes (such as the gravothermal catastrophe). However, globular clusters represent a tiny fraction of the baryonic mass in the local Universe ($\lesssim 1$ per cent, Harris *et al.* 2013).

In contrast, only few studies of BH binaries (e.g. Ziosi *et al.* 2014; Mapelli 2016; Kimpson *et al.* 2016; Banerjee 2017) focus on *young star clusters*. These young ($\lesssim 100$ Myr), relatively dense ($> 10^3 M_{\odot}$ pc $^{-3}$) stellar systems are thought to be the most common birthplace of massive stars. When they evaporate (by gas loss) or are disrupted by the tidal field of their host galaxy, their stellar content is released into the field. Thus, it is reasonable to expect that a large fraction of BH binaries which are now in the field may have formed in young star clusters, where they participated in the dynamics of the cluster. The reason why young star clusters have been neglected in the past is exquisitely numerical: the dynamics of young star clusters needs to be studied with direct N-body simulations, which are rather expensive (they scale as N^2), combined with population-synthesis simulations. Moreover, their dynamical evolution may be significantly affected by the presence of gas. Including gas would require a challenging interface between direct N-body simulations and hydrodynamical simulations, which has been done in very few cases (Moeckel & Bate 2010; Parker & Dale 2013; Fuji *et al.* 2015; Mapelli 2017) and has been never used to study BH binaries. Finally, a fraction of young star clusters might survive gas evaporation and tidal disruption and evolve into older *open clusters*, like M67.

Another flavour of star cluster where BH binaries might form and evolve dynamically are *nuclear star clusters*, i.e. star clusters which lie in the nuclei of galaxies. Nuclear star clusters are rather common in galaxies (e.g. Böker *et al.* 2002; Ferrarese *et al.* 2006; Graham *et al.* 2009), are usually more massive and denser than globular clusters, and may co-exist with super-massive BHs (SMBHs). Stellar-mass BHs formed in the innermost regions of a galaxy could even be “trapped” in the accretion disc of the central SMBH, triggering their merger (see e.g. Stone *et al.* 2016; Bartos *et al.* 2017; McKernan *et al.* 2017). These features make nuclear star clusters unique among star clusters, for the effects that we will describe in the next sections.

4.2. Three-body encounters

We now review what are the main dynamical effects which can affect a BH binary, starting from three-body encounters. Binaries have a energy reservoir, their internal energy:

$$E_{\text{int}} = \frac{1}{2} \mu v^2 - \frac{G m_1 m_2}{r}, \quad (4.1)$$

where $\mu = m_1 m_2 / (m_1 + m_2)$ is the reduced mass of the binary (whose components have mass m_1 and m_2), v is the relative velocity between the two members of the binary, and r is the distance between the two members of the binary. As shown by Kepler's laws, $E_{\text{int}} = -E_{\text{b}} = -G m_1 m_2 / (2a)$, where E_{b} is the binding energy of the binary (a being the semi-major axis of the binary).

The internal energy of a binary can be exchanged with other stars only if the binary undergoes a close encounter with a star, so that its orbital parameters are perturbed by the intruder. This happens only if a single star approaches the binary by few times its orbital separation. We define this close encounter between a binary and a single star as a *three-body encounter*. For this to happen with a non-negligible frequency, the binary must be in a dense environment, because the rate of three-body encounters scales with the local density of stars. Three-body encounters have crucial effects on BH binaries, such as *exchanges*, *hardening*, and *ejections*.

4.3. Exchanges

Dynamical exchanges are three-body encounters during which one of the former members of the binary is replaced by the intruder.

Exchanges may lead to the formation of new double BH binaries. If a binary composed of a BH and a low-mass star undergoes an exchange with a single BH, this leads to the formation of a new double BH binary. This is a very important difference between BHs in the field and in star clusters: a BH which forms as a single object in the field has negligible chances to become member of a binary system, while a single BH in the core of a star cluster has good chances of becoming member of a binary by exchanges.

Exchanges are expected to lead to the formation of many more double BH binaries than they can destroy, because the probability for an intruder to replace one of the members of a binary is ≈ 0 if the intruder is less massive than both binary members, while it suddenly jumps to ~ 1 if the intruder is more massive than one of the members of the binary (Hills & Fullerton 1980). Since BHs are among the most massive bodies in a star cluster (after their massive progenitors transform into them), they are very efficient in acquiring companions through dynamical exchanges.

Thus, exchanges are a crucial mechanism to form BH binaries dynamically. By means of direct N-body simulations, Ziosi *et al.* (2014) show that > 90 per cent of double BH binaries in young star clusters form by dynamical exchange.

Moreover, BH binaries formed via dynamical exchange will have some distinctive features with respect to field BH binaries:

- double BH binaries formed by exchanges will be (on average) more massive than isolated double BH binaries, because more massive intruders have higher chances to acquire companions;
- exchanges trigger the formation of highly eccentric double BH binaries (eccentricity is then significantly reduced by circularisation induced by GW emission, if the binary enters the regime where GW emission is effective);
- double BH binaries born by exchange will likely have misaligned spins, because exchanges tend to randomize the spins.

Spin misalignments are another possible feature to discriminate between field binaries and star cluster binaries (e.g. [Farr et al. 2017a,b](#)). Unfortunately, there is no robust theory to predict the magnitude of the spin of a BH given the spin of its parent star ([Miller & Miller 2015](#)). However, we can reasonably state that the orientation of the spin of a BH matches the orientation of the spin of its progenitor star, if the latter evolved in isolation and directly collapsed to a BH.

Thus, we expect that an isolated binary in which the secondary becomes a BH by direct collapse results in a double BH binary with aligned spins (i.e. the spins of the two BHs have the same orientation, which is approximately the same as the orbital angular momentum direction of the binary), because tidal evolution and mass transfer in a binary tend to synchronise the spins ([Hurley et al. 2002](#)). On the other hand, if the secondary undergoes a SN explosion, the natal kick may reshuffle spins.

For dynamically formed BH binaries (through exchange) we expect misaligned, or even nearly isotropic spins, because any original spin alignment is completely reset by three-body encounters.

4.4. Hardening

If a double BH binary undergoes a number of three-body encounters during its life, we expect that its semi-major axis will shrink as an effect of the encounters. This process is called dynamical *hardening*.

Following [Heggie \(1975\)](#), we call hard binaries (soft binaries) those binaries with binding energy larger (smaller) than the average kinetic energy of a star in the star cluster. According to Heggie's law (1975), hard binaries tend to harden (i.e. to become more and more bound) via three-body encounters. In other words, a fraction of the internal energy of a hard binary can be transferred into kinetic energy of the intruders and of the centre-of-mass of the binary during three body encounters. This means that the binary loses internal energy and its semi-major axis shrinks.

Most double BH binaries are expected to be hard binaries, because BHs are among the most massive bodies in star clusters. Thus, double BH binaries are expected to harden as a consequence of three-body encounters. The hardening process may be sufficiently effective to shrink a BH binary till it enters the regime where GW emission is efficient: a BH binary which is initially too loose to merge may then become a GW source thanks to dynamical hardening.

It is even possible to make a simple analytic estimate of the evolution of the semi-major axis of a double BH binary which is affected by three-body encounters and by GW emission (equation 9 of [Colpi et al. 2003](#)):

$$\frac{da}{dt} = -2\pi\zeta \frac{G\rho}{\sigma} a^2 - \frac{64}{5} \frac{G^3 m_1 m_2 (m_1 + m_2)}{c^5 (1 - e^2)^{7/2}} a^{-3}, \quad (4.2)$$

where $\zeta \sim 0.2 - 1$ is a dimensionless hardening parameter (which has been estimated through numerical experiments, [Hills 1983](#)), ρ is the local mass density of stars, σ is the local velocity dispersion, c is the light speed, e is the eccentricity. The first part of the right-hand term of equation 4.2 accounts for the effect of three-body hardening on the semi-major axis. It scales as $da/dt \propto -a^2$, indicating that the wider the binary is, the more effective the hardening. This can be easily understood considering that the geometric cross section for three body interactions with a binary scales as a^2 .

The second part of the right-hand term of equation 4.2 accounts for energy loss by GW emission. It is the first-order approximation of the calculation by ([Peters 1964](#)). It scales as $da/dt \propto -a^{-3}$ indicating that GW emission becomes efficient only when the two BHs are very close to each other.

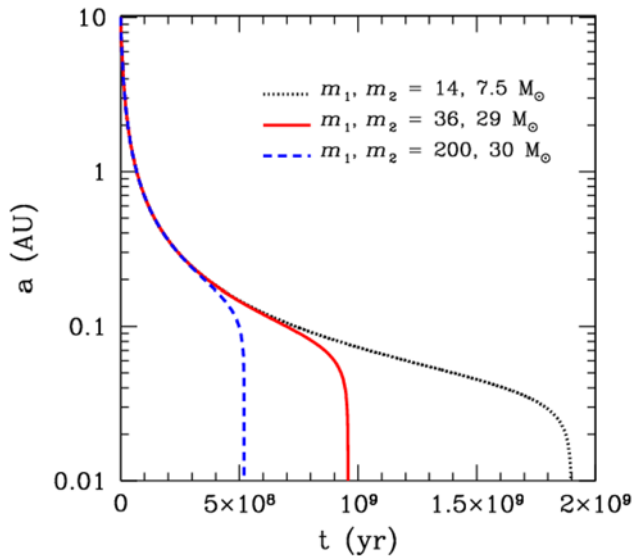


Figure 5. Time evolution of the semi-major axis of three BH binaries estimated from equation 4.2. Blue dashed line: BH binary with masses $m_1 = 200 M_\odot$, $m_2 = 30 M_\odot$; red solid line: $m_1 = 36 M_\odot$, $m_2 = 29 M_\odot$; black dotted line: $m_1 = 14 M_\odot$, $m_2 = 7.5 M_\odot$. For all BH binaries: $\xi = 1$, $\rho = 10^5 M_\odot \text{pc}^{-3}$, $\sigma = 10 \text{ km s}^{-1}$, $e = 0$ (here we assume that ρ , σ and e do not change during the evolution), initial semi-major axis of the BH binary $a_i = 10 \text{ AU}$.

In Figure 5 we solve equation 4.2 numerically for three double BH binaries with different mass. All binaries evolve through (i) a first phase in which hardening by three body encounters dominates the evolution of the binary, (ii) a second phase in which the semi-major axis stalls because three-body encounters become less efficient as the semi-major axis shrink, but the binary is still too wide for GW emission to become efficient, and (iii) a third phase in which the semi-major axis drops because the binary enters the regime where GW emission is efficient.

4.5. Formation of intermediate-mass black holes by runaway collisions

In Section 2.3, we have mentioned that intermediate-mass black holes (IMBHs, i.e. BHs with mass $100 \lesssim m_{\text{BH}} \lesssim 10^4 M_\odot$) might form from the direct collapse of metal-poor extremely massive stars (Spera & Mapelli 2017). Other formation channels have been proposed for IMBHs and most of them involve dynamics of star clusters. The formation of massive BHs by runaway collisions has been originally proposed about half a century ago (Colgate 1967; Sanders 1970) and was then elaborated by several authors (e.g. Portegies Zwart *et al.* 1999; Portegies Zwart & McMillan 2002; Portegies Zwart *et al.* 2004, Gürkan *et al.* 2006; Freitag *et al.* 2006; Mapelli *et al.* 2006, 2008; Giersz *et al.* 2015; Mapelli 2016).

The basic idea is the following (as summarized by the cartoon in Figure 6). In a dense star cluster, dynamical friction (Chandrasekhar 1943) makes massive stars to decelerate because of the drag exerted by lighter bodies, on a timescale which can be expressed as

$$t_{\text{DF}}(M) = \frac{\langle m \rangle}{M} t_{\text{rlx}}, \quad (4.3)$$

where $\langle m \rangle$ is the average star mass in a star cluster (for young star clusters $\langle m \rangle \sim 1 M_\odot$), M is the mass of the massive star we consider ($M > \langle m \rangle$) and t_{rlx} is the central two body relaxation timescale of the star cluster (i.e. the timescale needed for a star to

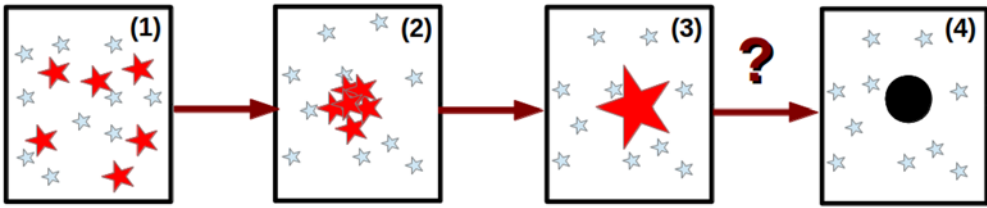


Figure 6. Cartoon of the runaway collision scenario in dense young star clusters (see e.g. [Portegies Zwart & McMillan 2002](#)). From left to right: (1) the massive stars (red big stars) and the low-mass stars (blue small stars) follow the same initial spatial distribution; (2) dynamical friction leads the massive stars to sink to the core of the cluster, where they start colliding between each other; (3) a very massive star ($\gg 100 M_{\odot}$) forms as a consequence of the runaway collisions; (4) this massive star might be able to directly collapse into a BH.

completely lose memory of its initial velocity as an effect of two-body encounters, [Spitzer *et al.* 1971](#)). For dense young star clusters

$$t_{\text{rlx}} \simeq 20 \text{ Myr} \left(\frac{M_{\text{cl}}}{10^4 M_{\odot}} \right)^{1/2} \left(\frac{R_{\text{cl}}}{1 \text{ pc}} \right)^{3/2} \left(\frac{M_{\odot}}{\langle m \rangle} \right), \quad (4.4)$$

where M_{cl} is the total star cluster mass and R_{cl} is the virial radius of the star cluster ([Portegies Zwart *et al.* 2010](#)).

Thus, for a star with mass $M \geq 25 M_{\odot}$, we estimate $t_{\text{DF}} \leq 1 \text{ Myr}$: dynamical friction is very effective in dense massive young star clusters. Because of dynamical friction, massive stars segregate to the core of the cluster, which is the centre of the cluster potential well.

If the most massive stars in a dense young star cluster sink to the centre of the cluster by dynamical friction on a time shorter than their lifetime (i.e. before core-collapse SNe take place, removing a large fraction of their mass), then the density of massive stars in the cluster core becomes extremely high. This makes collisions between massive stars extremely likely. Actually, direct N-body simulations show that collisions between massive stars proceed in a runaway sense, leading to the formation of a very massive ($\gg 100 M_{\odot}$) star ([Portegies Zwart & McMillan 2002](#)). The main open question is: ‘‘What is the final mass of the collision product? Is the collision product going to collapse to an IMBH?’’.

There are essentially two critical issues: (i) how much mass is lost during the collisions? (ii) how much mass does the very-massive star lose by stellar winds?

Hydrodynamical simulations of colliding stars ([Gaburov *et al.* 2008, 2010](#)) show that massive star can lose ≈ 25 per cent of their mass during collisions. Even if we optimistically assume that no mass is lost during and immediately after the collision (when the collision product relaxes to a new equilibrium), the resulting very massive star will be strongly radiation pressure dominated and is expected to lose a significant fraction of its mass by stellar winds. Recent studies including the effect of the Eddington factor on mass loss (e.g. [Mapelli 2016](#)) show that IMBHs cannot form from runaway collisions at solar metallicity. At lower metallicity ($Z \lesssim 0.1 Z_{\odot}$) approximately 10 – 30 per cent of runaway collision products in young dense star clusters can become IMBHs by direct collapse (they also avoid being disrupted by pair-instability SNe).

Other possible formation channels of IMBHs include the repeated merger scenario ([Miller & Hamilton 2002; Giersz *et al.* 2015](#)) and the formation by gas drag in galactic nuclei ([Miller & Davies 2012; McKernan *et al.* 2012, 2014; Stone *et al.* 2017](#)).

4.6. Kozai-Lidov resonance

Unlike the other dynamical processes discussed so far, Kozai-Lidov (KL) resonance ([Kozai 1962; Lidov 1962](#)) can occur both in the field and in star clusters. KL resonance appears whenever we have a stable hierarchical triple system (i.e. a triple composed of an

inner binary and an outer body orbiting the inner binary), in which the orbital plane of the outer body is inclined with respect to the orbital plane of the inner binary. Periodic perturbations induced by the outer body on the inner binary cause (i) the eccentricity of the inner binary and (ii) the inclination between the orbital plane of the inner binary and that of the outer body to oscillate.

KL oscillations may enhance BH binary mergers because the timescale for merger by GW emission strongly depends on the eccentricity e of the binary (Peters 1964).

It might seem that hierarchical triples are rather exotic systems. This is not the case. In fact, ~ 10 per cent of low-mass stars are in triple systems (Tokovinin *et al.* 2008; Raghavan *et al.* 2010). This fraction gradually increases for more massive stars, up to ~ 50 per cent for B-type stars (Sana *et al.* 2014; Moe & Di Stefano 2016).

The main signature of the merger of a KL system is the non-zero eccentricity until very few seconds before the merger. Eccentricity might be significantly non-zero even when the system enters the LIGO-Virgo frequency range (e.g. Toonen *et al.* 2017; Antonini *et al.* 2017).

4.7. Summary of dynamics

In this section, we have seen that dynamics is a crucial ingredient to understand BH demography. Dynamical interactions (three and few body close encounters) can favour the coalescence of BH binaries through dynamical hardening. New BH binaries can form via dynamical exchanges. Both processes suggest a boost of the BH binary merger rate in a dynamically active environment.

Moreover, exchanges favour the formation of more massive binaries, with higher initial eccentricity and with misaligned spins. Also, KL resonances favour the coalescence of more massive binaries and with higher eccentricity, even close to the last stable orbit. On the other hand, three-body encounters might trigger the ejection of compact-object binaries from their natal environment, inducing a significant displacement between the birth place of the binary and the location of its merger. Finally, dynamics can lead to the formation of IMBHs, with mass of few hundreds solar masses.

The right-hand panel of Figure 4 summarizes one of the possible evolutionary pathways of merging BHBs which originate from dynamics (the variety of this formation channel is too large to account for all dynamical channels mentioned above in a single cartoon). As in the isolated binary case, we start from a stellar binary. In the dynamical scenario, it is not important that this binary evolves through Roche lobe or CE (although this may happen). After the primary has turned into a BH, the binary undergoes a dynamical exchange: the secondary is replaced by a massive BH and a new BHB forms. The new binary is not ejected from the star cluster and undergoes further three-body encounters. As an effect of these three-body encounters the binary hardens enough to enter the regime in which GW emission is efficient: the BHB merges by GW decay.

5. Summary and outlook

We reviewed our current understanding of the astrophysics of stellar-mass BHs. The era of gravitational wave astrophysics has just begun and has already produced two formidable results: BH binaries exist and can host BHs with mass $> 30 M_{\odot}$ (Abbott *et al.* 2016a,d, 2018a).

According to nowadays stellar evolution and supernova theories, such massive BHs can form only from massive relatively metal-poor stars. At low-metallicity, stellar winds are quenched and stars end their life with a larger mass than their metal-rich analogues. If its final mass and its final core mass are sufficiently large, a star can directly collapse to a BH with mass $\gtrsim 30 M_{\odot}$ (Mapelli *et al.* 2009; Belczynski *et al.* 2010). An alternative

scenario predicts that $\sim 30 - 40 M_{\odot}$ BHs are the result of gravitational instabilities in the very early Universe (primordial BHs, e.g. Carr *et al.* 2016).

The formation channels of merging BH binaries are still an open question. All proposed scenarios have several drawbacks and uncertainties. While mass transfer and common envelope are a major issue in the isolated binary evolution scenario, even the dynamical evolution is still effected by major issues (e.g. the small statistics about BHs in young star clusters, and the major simplifications adopted in dynamical simulations).

Finally, a global picture is missing, which combines stellar and binary evolution with dynamics and cosmology, aimed at reconstructing the BH merger history across cosmic time. This is crucial for the astrophysical interpretation of LIGO-Virgo data and for meeting the challenge of third-generation ground-based GW detectors.

Acknowledgements

MM acknowledges financial support by the European Research Council for the ERC Consolidator grant DEMOBLACK, under contract no. 770017. This review is based on the material of the lecture I held for the Course 200 on “Gravitational Waves and Cosmology” of the International School of Physics “Enrico Fermi”. This work benefited from support by the International Space Science Institute (ISSI), Bern, Switzerland, through its International Team programme ref. no. 393 *The Evolution of Rich Stellar Populations & BH Binaries* (2017-18).

References

- Abbott, B. P., Abbott, R., Abbott, T. D., *et al.* 2016, Physical Review Letters, 116, 061102
 Abbott, B. P., Abbott, R., Abbott, T. D., *et al.* 2016, Physical Review Letters, 116, 241103
 Abbott, B. P., Abbott, R., Abbott, T. D., *et al.* 2017, Physical Review Letters, 118, 221101
 Abbott, B. P., Abbott, R., Abbott, T. D., *et al.* 2017, Astrophysical Journal Letter, 851, L35
 Abbott, B. P., Abbott, R., Abbott, T. D., *et al.* 2017, Physical Review Letters, 119, 141101
 Abbott, B. P., Abbott, R., Abbott, T. D., *et al.* 2016, Physical Review X, 6, 041015
 The LIGO Scientific Collaboration, & the Virgo Collaboration 2018, [arXiv:1811.12907](https://arxiv.org/abs/1811.12907)
 The LIGO Scientific Collaboration, & The Virgo Collaboration 2018, [arXiv:1811.12940](https://arxiv.org/abs/1811.12940)
 Aasi, J., Abadie, J., Abbott, B. P., *et al.* 2015, Classical and Quantum Gravity, 32, 115012
 Acernese, F., Agathos, M., Agatsuma, K., *et al.* 2015, Classical and Quantum Gravity, 32, 024001
 Abbott, B. P., Abbott, R., Abbott, T. D., *et al.* 2016, Astrophysical Journal Letter, 818, L22
 Tutukov, A., & Yungelson, L. 1973, Nauchnye Informatsii, 27, 70
 Thorne, K. S. 1987, Three Hundred Years of Gravitation, 330
 Schutz, B. F. 1989, Classical and Quantum Gravity, 6, 1761
 Kulkarni, S. R., Hut, P., & McMillan, S. 1993, Nature, 364, 421
 Sigurdsson, S., & Hernquist, L. 1993, Nature, 364, 423
 Bethe, H. A., & Brown, G. E. 1998, Astrophysical Journal, 506, 780
 Portegies Zwart, S. F., & McMillan, S. L. W. 2000, Astrophysical Journal Letter, 528, L17
 Colpi, M., Mapelli, M., & Possenti, A. 2003, Astrophysical Journal, 599, 1260
 Belczynski, K., Sadowski, A., & Rasio, F. A. 2004, Astrophysical Journal, 611, 1068
 Mapelli, M., Colpi, M., & Zampieri, L. 2009, MNRAS, 395, L71
 Mapelli, M., Ripamonti, E., Zampieri, L., Colpi, M., & Bressan, A. 2010, MNRAS, 408, 234
 Belczynski, K., Bulik, T., Fryer, C. L., *et al.* 2010, Astrophysical Journal, 714, 1217
 Fryer, C. L., Belczynski, K., Wiktorowicz, G., *et al.* 2012, Astrophysical Journal, 749, 91
 Mapelli, M., Zampieri, L., Ripamonti, E., & Bressan, A. 2013, MNRAS, 429, 2298
 Ziosi, B. M., Mapelli, M., Branchesi, M., & Tormen, G. 2014, MNRAS, 441, 3703
 Spera, M., Mapelli, M., & Bressan, A. 2015, MNRAS, 451, 4086
 Bird, S., Cholis, I., Muñoz, J. B., *et al.* 2016, Physical Review Letters, 116, 201301
 Carr, B., Kühnel, F., & Sandstad, M. 2016, Physical Review Documents, 94, 083504

- Inomata, K., Kawasaki, M., Mukaida, K., Tada, Y., & Yanagida, T. T. 2017, *Physical Review Documents*, 95, 123510
- van Loon, J. T., Cioni, M.-R. L., Zijlstra, A. A., & Loup, C. 2005, *Astronomy & Astrophysics*, 438, 273
- Orosz, J. A. 2003, *A Massive Star Odyssey: From Main Sequence to Supernova*, 212, 365
- Özel, F., Psaltis, D., Narayan, R., & McClintock, J. E. 2010, *Astrophysical Journal*, 725, 1918
- Laycock, S. G. T., Maccarone, T. J., & Christodoulou, D. M. 2015, *MNRAS*, 452, L31
- Fryer, C. L. 1999, *Astrophysical Journal*, 522, 413
- Fryer, C. L., & Kalogera, V. 2001, *Astrophysical Journal*, 554, 548
- Abbott, D. C. 1982, *Astrophysical Journal*, 259, 282
- Kudritzki, R. P., Pauldrach, A., & Puls, J. 1987, *Astronomy & Astrophysics*, 173, 293
- Leitherer, C., Robert, C., & Drissen, L. 1992, *Astrophysical Journal*, 401, 596
- Vink, J. S., de Koter, A., & Lamers, H. J. G. L. M. 2001, *Astronomy & Astrophysics*, 369, 574
- Kudritzki, R.-P., & Puls, J. 2000, *Annual Review of Astronomy and Astrophysics*, 38, 613
- Vink, J. S., & de Koter, A. 2005, *Astronomy & Astrophysics*, 442, 587
- Hainich, R., Pasemann, D., Todt, H., *et al.* 2015, *Astronomy & Astrophysics*, 581, A21
- Gräfener, G., & Hamann, W.-R. 2008, *Astronomy & Astrophysics*, 482, 945
- Gräfener, G., Vink, J. S., de Koter, A., & Langer, N. 2011, *Astronomy & Astrophysics*, 535, A56
- Vink, J. S., Muijres, L. E., Anthonisse, B., *et al.* 2011, *Astronomy & Astrophysics*, 531, A132
- Chen, Y., Bressan, A., Girardi, L., *et al.* 2015, *MNRAS*, 452, 1068
- Janka, H.-T. 2012, *Annual Review of Nuclear and Particle Science*, 62, 407
- Foglizzo, T., Kazeroni, R., Guilet, J., *et al.* 2015, *Publications of the Astronomical Society of Australia*, 32, e009
- Ertl, T., Janka, H.-T., Woosley, S. E., Sukhbold, T., & Ugliano, M. 2016, *Astrophysical Journal*, 818, 124
- Müller, B., Janka, H.-T., & Marek, A. 2012, *Astrophysical Journal*, 756, 84
- Müller, B., Janka, H.-T., & Heger, A. 2012, *Astrophysical Journal*, 761, 72
- O'Connor, E., & Ott, C. D. 2011, *Astrophysical Journal*, 730, 70
- Ugliano, M., Janka, H.-T., Marek, A., & Arcones, A. 2012, *Astrophysical Journal*, 757, 69
- Horiuchi, S., Nakamura, K., Takiwaki, T., Kotake, K., & Tanaka, M. 2014, *MNRAS*, 445, L99
- Sukhbold, T., & Woosley, S. E. 2014, *Astrophysical Journal*, 783, 10
- Sukhbold, T., Ertl, T., Woosley, S. E., Brown, J. M., & Janka, H.-T. 2016, *Astrophysical Journal*, 821, 38
- Fowler, W. A., & Hoyle, F. 1964, *Astrophysical Journal Supplement*, 9, 201
- Barkat, Z., Rakavy, G., & Sack, N. 1967, *Physical Review Letters*, 18, 379
- Rakavy, G., & Shaviv, G. 1967, *Astrophysical Journal*, 148, 803
- Woosley, S. E. 2017, *Astrophysical Journal*, 836, 244
- Heger, A., & Woosley, S. E. 2002, *Astrophysical Journal*, 567, 532
- Heger, A., Woosley, S. E., Fryer, C. L., & Langer, N. 2003, *From Twilight to Highlight: The Physics of Supernovae*, 3
- Spera, M., & Mapelli, M. 2017, *MNRAS*, 470, 4739
- Fishbach, M., & Holz, D. E. 2017, *Astrophysical Journal Letter*, 851, L25
- Talbot, C., & Thrane, E. 2018, *Astrophysical Journal*, 856, 173
- Wysocki, D., Lange, J., & O'Shaughnessy, R. 2018, [arXiv:1805.06442](https://arxiv.org/abs/1805.06442)
- Giacobbo, N., & Mapelli, M. 2019, *MNRAS*, 482, 2234
- Portegies Zwart, S. F., & Verbunt, F. 1996, *Astronomy & Astrophysics*, 309, 179
- Hurley, J. R., Tout, C. A., & Pols, O. R. 2002, *MNRAS*, 329, 897
- Podsiadlowski, P., Rappaport, S., & Han, Z. 2003, *MNRAS*, 341, 385
- Belczynski, K., Kalogera, V., Rasio, F. A., *et al.* 2008, *Astrophysical Journal Supplement*, 174, 223
- Mennekens, N., & Vanbeveren, D. 2014, *Astronomy & Astrophysics*, 564, A134
- Eldridge, J. J., & Stanway, E. R. 2016, *MNRAS*, 462, 3302
- Mapelli, M., Giacobbo, N., Ripamonti, E., & Spera, M. 2017, *MNRAS*, 472, 2422

- Stevenson, S., Vigna-Gómez, A., Mandel, I., *et al.* 2017, *Nature Communications*, 8, 14906
- Giacobbo, N., Mapelli, M., Ripamonti, E., Spera, M. 2018, *MNRAS*, 474, 2959
- Barrett, J. W., Gaebel, S. M., Neijssel, C. J., *et al.* 2018, *MNRAS*, 477, 4685
- Giacobbo, N., Mapelli, M. 2018, *MNRAS*, 480, 2011
- Mapelli, M., Giacobbo, N. 2018, *MNRAS*, 479, 4391
- Kruckow, M. U., Tauris, T. M., Langer, N., Kramer, M., & Izzard, R. G. 2018, [arXiv:1801.05433](https://arxiv.org/abs/1801.05433)
- Eldridge, J. J., Stanway, E. R., & Tang, P. N. 2018, [arXiv:1807.07659](https://arxiv.org/abs/1807.07659)
- Spera, M., Mapelli, M., Giacobbo, N., *et al.* 2018, [arXiv:1809.04605](https://arxiv.org/abs/1809.04605)
- Eggleton, P. P. 1983, *Astrophysical Journal*, 268, 368
- Esposito, P., Israel, G. L., Milisavljevic, D., *et al.* 2015, *MNRAS*, 452, 1112
- Webbink, R. F. 1984, *Astrophysical Journal*, 277, 355
- Ivanova, N., Justham, S., Chen, X., *et al.* 2013, *The Astronomy and Astrophysics Review*, 21, 59
- de Mink, S. E., & Mandel, I. 2016, *MNRAS*, 460, 3545
- Mandel, I., & de Mink, S. E. 2016, *MNRAS*, 458, 2634
- Marchant, P., Langer, N., Podsiadlowski, P., Tauris, T. M., & Moriya, T. J. 2016, *Astronomy & Astrophysics*, 588, A50
- Hainich, R., Oskinova, L. M., Shenar, T., *et al.* 2018, *Astronomy & Astrophysics*, 609, A94
- Belczynski, K., Holz, D. E., Bulik, T., & O'Shaughnessy, R. 2016, *Nature*, 534, 512
- Lada, C. J., & Lada, E. A. 2003, *Annual Review of Astronomy and Astrophysics*, 41, 57
- Weidner, C., & Kroupa, P. 2006, *MNRAS*, 365, 1333
- Weidner, C., Kroupa, P., & Bonnell, I. A. D. 2010, *MNRAS*, 401, 275
- Portegies Zwart, S. F., McMillan, S. L. W., & Gieles, M. 2010, *Annual Review of Astronomy and Astrophysics*, 48, 431
- Mapelli, M., Colpi, M., Possenti, A., & Sigurdsson, S. 2005, *MNRAS*, 364, 1315
- Downing, J. M. B., Benacquista, M. J., Giersz, M., & Spurzem, R. 2010, *MNRAS*, 407, 1946
- Benacquista, M. J., & Downing, J. M. B. 2013, *Living Reviews in Relativity*, 16, 4
- Samsing, J., MacLeod, M., & Ramirez-Ruiz, E. 2014, *Astrophysical Journal*, 784, 71
- Rodriguez, C. L., Morscher, M., Pattabiraman, B., *et al.* 2015, *Physical Review Letters*, 115, 051101
- Rodriguez, C. L., Chatterjee, S., & Rasio, F. A. 2016, *Physical Review Documents*, 93, 084029
- Askar, A., Szkudlarek, M., Gondek-Rosińska, D., Giersz, M., & Bulik, T. 2017, *MNRAS*, 464, L36
- Samsing, J., Askar, A., & Giersz, M. 2018, *Astrophysical Journal*, 855, 124
- Harris, W. E., Harris, G. L. H., & Alessi, M. 2013, *Astrophysical Journal*, 772, 82
- Mapelli, M. 2016, *MNRAS*, 459, 3432
- Kimpson, T. O., Spera, M., Mapelli, M., & Ziosi, B. M. 2016, *MNRAS*, 463, 2443
- Banerjee, S. 2017, *MNRAS*, 467, 524
- Moeckel, N., & Bate, M. R. 2010, *MNRAS*, 404, 721
- Parker, R. J., & Dale, J. E. 2013, *MNRAS*, 432, 986
- Fujii, M. S., & Portegies Zwart, S. 2015, *MNRAS*, 449, 726
- Mapelli, M. 2017, *MNRAS*, 467, 3255
- Böker, T., Laine, S., van der Marel, R. P., *et al.* 2002, *Astronomical Journal*, 123, 1389
- Ferrarese, L., Côté, P., Dalla Bontà, E., *et al.* 2006, *Astrophysical Journal Letter*, 644, L21
- Graham, A. W., & Spitler, L. R. 2009, *MNRAS*, 397, 2148
- Stone, N. C., Metzger, B. D., & Haiman, Z. 2017, *MNRAS*, 464, 946
- Bartos, I., Kocsis, B., Haiman, Z., & Márka, S. 2017, *Astrophysical Journal*, 835, 165
- McKernan, B., Ford, K. E. S., Bellovary, J., *et al.* 2017, [arXiv:1702.07818](https://arxiv.org/abs/1702.07818)
- Hills, J. G., & Fullerton, L. W. 1980, *Astronomical Journal*, 85, 1281
- Farr, W. M., Stevenson, S., Miller, M. C., *et al.* 2017, *Nature*, 548, 426
- Farr, B., Holz, D. E., & Farr, W. M. 2018, *Astrophysical Journal Letter*, 854, L9
- Miller, M. C., & Miller, J. M. 2015, *Physics Reports*, 548, 1
- Heggie, D. C. 1975, *MNRAS*, 173, 729
- Hills, J. G. 1983, *Astronomical Journal*, 88, 1269

- Peters, P. C. 1964, *Physical Review*, 136, 1224
- Colgate, S. A. 1967, *Astrophysical Journal*, 150, 163
- Sanders, R. H. 1970, *Astrophysical Journal*, 162, 791
- Portegies Zwart, S. F., Makino, J., McMillan, S. L. W., & Hut, P. 1999, *Astronomy & Astrophysics*, 348, 117
- Portegies Zwart, S. F., & McMillan, S. L. W. 2002, *Astrophysical Journal*, 576, 899
- Portegies Zwart, S. F., Baumgardt, H., Hut, P., Makino, J., & McMillan, S. L. W. 2004, *Nature*, 428, 724
- Gürkan, M. A., Fregeau, J. M., & Rasio, F. A. 2006, *Astrophysical Journal Letter*, 640, L39
- Freitag, M., Gürkan, M. A., & Rasio, F. A. 2006, *MNRAS*, 368, 141
- Mapelli, M., Ferrara, A., & Rea, N. 2006, *MNRAS*, 368, 1340
- Mapelli, M., Moore, B., Giordano, L., *et al.* 2008, *MNRAS*, 383, 230
- Giersz, M., Leigh, N., Hypki, A., Lützgendorf, N., & Askar, A. 2015, *MNRAS*, 454, 3150
- Chandrasekhar, S. 1943, *Astrophysical Journal*, 97, 255
- Spitzer, L., Jr., & Hart, M. H. 1971, *Astrophysical Journal*, 164, 399
- Gaburov, E., Lombardi, J. C., & Portegies Zwart, S. 2008, *MNRAS*, 383, L5
- Gaburov, E., Lombardi, J. C., Jr., & Portegies Zwart, S. 2010, *MNRAS*, 402, 105
- Miller, M. C., & Hamilton, D. P. 2002, *MNRAS*, 330, 232
- Miller, M. C., & Davies, M. B. 2012, *Astrophysical Journal*, 755, 81
- Stone, N. C., Küpper, A. H. W., & Ostriker, J. P. 2017, *MNRAS*, 467, 4180
- McKernan, B., Ford, K. E. S., Lyra, W., & Perets, H. B. 2012, *MNRAS*, 425, 460
- McKernan, B., Ford, K. E. S., Kocsis, B., Lyra, W., & Winter, L. M. 2014, *MNRAS*, 441, 900
- Kozai, Y. 1962, *Astronomical Journal*, 67, 591
- Lidov, M. L. 1962, *Planetary and Space Science*, 9, 719
- Tokovinin, A. 2008, *MNRAS*, 389, 925
- Raghavan, D., McAlister, H. A., Henry, T. J., *et al.* 2010, *Astrophysical Journal Supplement*, 190, 1
- Sana, H., Le Bouquin, J.-B., Lacour, S., *et al.* 2014, *Astrophysical Journal Supplement*, 215, 15
- Moe, M., & Di Stefano, R. 2017, *Astrophysical Journal Supplement*, 230, 15
- Toonen, S., Hamers, A., & Portegies Zwart, S. 2016, *Computational Astrophysics and Cosmology*, 3, 6
- Antonini, F., Toonen, S., & Hamers, A. S. 2017, *Astrophysical Journal*, 841, 77